Digest Journal of Nanomaterials and Biostructures Vol. 9, No. 2, April – June 2014, p. 593 - 598

SYNTHESIS OF Bi_2MoO_6 NANOPLATES WITH THE ASSISTANCE OF PEG BY HYDROTHERMAL METHOD AND THEIR PHOTOCATALYTIC ACTIVITIES

P. DUMRONGROJTHANATH[a], T. THONGTEM[a*], A. PHURUANGRAT[b*]
S. THONGTEM[c,d]
[a] *Department of Chemistry, Faculty of Science, Chiang Mai University, Chiang Mai 50200, Thailand*
[b] *Department of Materials Science and Technology, Faculty of Science, Prince of Songkla University, Hat Yai, Songkhla 90112, Thailand*
[c] *Department of Physics and Materials Science, Faculty of Science, Chiang Mai University, Chiang Mai 50200, Thailand*
[d] *Materials Science Research Center, Faculty of Science, Chiang Mai University, Chiang Mai 50200, Thailand*

Bi_2MoO_6 nanoplates have been successfully synthesized via a simple hydrothermal method using polyethylene glycol (PEG) with M.W. of 20,000 as surfactant. The as-synthesized products have been characterized by X-ray diffraction, Raman spectroscopy, scanning electron microscopy and transmission electron microscopy. In this research, the results show that the as-synthesized products were orthorhombic Bi_2MoO_6 phase. The photocatalytic activity was tested using tetraethylated rhodamine B (RhB) degradation under UV visible light. The photocatalytic activity of Bi_2MoO_6 nanoplates was determined to be 95.02 % RhB degradation within 100 min irradiation time.

(Received January 29, 2014; Accepted April 23, 2014)

Keywords: Hydrothermal synthesis; X-ray diffraction; Electron microscopy; Spectroscopy

1. Introduction

In the past two decades, the researchers have focused on the photocatalytic properties of semiconducting materials because of their wide applications in solar energy conversion, environmental purification and others [1–3]. Among them, TiO_2 is the most extensive interest due to its chemical stability, strong oxidation activity, nontoxicity and economic efficiency. However, the relatively wide band gap (E_g = 3.0–3.2 eV) restricts the TiO_2 photosensitivity only in the ultraviolet (UV) region. Mostly it can only be excited by UV irradiation (4% of solar spectrum) [1–5]. Therefore, the development of new and efficient visible-light-driven photocatalyst (46 % of solar spectrum) [6] are the major challenge.

Bismuth molybdate is an excellent visible-light-driven photocatalytic activity for water splitting and decomposition of organic pollutants [3]. It has the chemical formula $Bi_2O_3.nMoO_3$ where n = 1, 2 or 3, corresponding to α-$Bi_2Mo_2O_9$, β-$Bi_2Mo_3O_{12}$ and γ-Bi_2MoO_6 [7–9]. Among these, γ-Bi_2MoO_6 has been found to accelerate reaction with the assisting of visible light for water splitting and organic pollutant degradation [7]. γ-Bi_2MoO_6, as an Aurivillius-phase perovskite, belongs to bismuth oxide family with the structure consisting of perovskite layers between bismuth oxide layers with a general formula of $[Bi_2O_2][A_{n-1}B_nO_{3n+1}]$ [10, 11]. It has been found that γ-Bi_2MoO_6 can be used as an ionic conductor, catalyst for CO conversion, catalyst for the selective oxidation and ammoxidation of lower olefin and visible-light responsive photocatalyst for the degradation of organic pollutants [7–11].

*Corresponding authors: phuruangrat@hotmail.com

In this research, visible-light-driven photocatalytic γ-Bi_2MoO_6 nanoplates were synthesized by hydrothermal reaction of solutions with different contents of PEG (MW =20,000). The effect of PEG on phase, morphology and photocatalytic performance was reported.

2. Experiment

Each 0.0025 mole of ammonium molybdate ($(NH_4)_6Mo_7O_{24}$) was dissolved in 20 ml deionized water to form four solutions. Following the dissolving process, 0.1, 0.3 and 0.5 g polyethylene glycol (PEG, M.W. = 20,000) were added to each of the solutions, excluding one was left as PEG-free. Concurrently, 0.0005 mole of $Bi(NO_3)_3 \cdot 5H_2O$ was dissolved in 15 ml 2M HNO_3 to form four solutions as well. The 20 ml and 15 ml solutions were mixed together under continuously stirring at room temperature. The mixtures were adjusted their pH to 9 by 28 % NH_4OH. Subsequently, they were hydrothermally processed at 180 ^oC for 24 h. In the end, the precipitates were separated by filtration, rinsed with distilled water and ethanol, and dried at 80 ^oC for 24 h for further characterization by X-ray diffraction, Raman spectroscopy, scanning electron microscopy, transmission electron microscopy, photocatalysis and UV-visible spectroscopy.

To evaluate photocatalysis, 500 mg of the product was added to 100 ml 10^{-5} M tetraethylated rhodamine (RhB) aqueous solution, which was stirred for 60 min in the dark environment to establish adsorption/desorption equilibrium. Photocatalysis was initiated by irradiation with UV light. Absorbance of the solutions was measured by UV-visible spectrophotometry at 553 nm wavelength for further calculation of decolorization efficiency (%) or $\frac{C_o - C_t}{C_o}$ x 100, where C_o and C_t were the concentrations of RhB before and after photocatalysis for different lengths of time, respectively.

3. Results and discussion

All XRD patterns of the as-synthesized products shown in Fig. 1(a) were indexed to orthorhombic Bi_2MoO_6 on according to the JCPDS database no. 21-0102 [12]. No impurities such as Bi_2O_3, MoO_3, and others were detected in the XRD patterns of the products. It should be noted that the relative intensity ratio based on the (060)/(131) peaks of Bi_2MoO_6 with 0.5 g PEG adding was two times higher than that of Bi_2MoO_6 without PEG. It indicates that the crystalline Bi_2MoO_6 unit cells with PEG would grow along the (0b0) direction and formed two dimensional product particles [13].

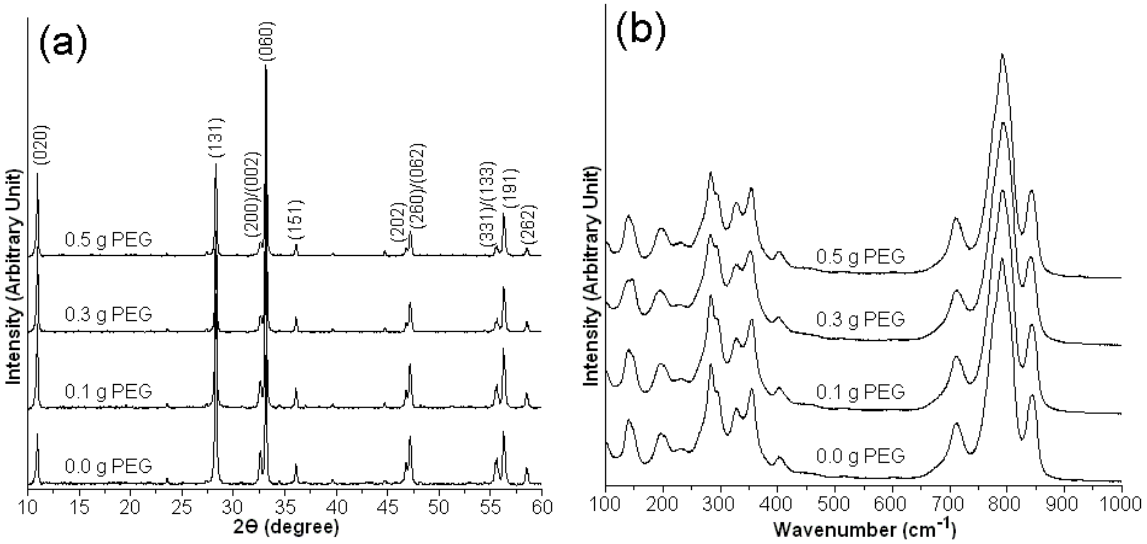

Fig. 1 (a) XRD patterns and (b) Raman spectra of Bi_2MoO_6 hydrothermally synthesized in the solutions containing 0.0, 0.1, 0.3 and 0.5 g PEG.

Raman spectra of Bi_2MoO_6 products shown in Fig. 1b present the peak below 180 cm^{-1} assigned to the translation of molybdenum and bismuth atoms. The peak at 144.18 cm^{-1} is assigned to the lattice mode of Bi^{3+} atoms mainly in the direction perpendicular to the layers. The intense Raman modes near 290 cm^{-1} and 280 cm^{-1} likely originate from the E_g mode bending vibration. The band at 323, 345.15 and 397.94 cm^{-1} correspond to the E_u symmetry bending modes. The 712 cm^{-1} mode is an asymmetric E_u stretching vibration. The Raman shifts mainly at 792.79 cm^{-1} (A_{1g} mode) and 839.65 cm^{-1} (A_{2u} mode) were assigned to the symmetric and asymmetric stretching vibrations of the WO_6 octahedrons [6, 9, 13, 14].

Fig. 2 shows SEM images of the as-synthesized Bi_2MoO_6 products. For the as-synthesized product in PEG-free solution, SEM image shows non-uniform microplates Bi_2MoO_6 structure. While in the presence of PEG, the non-uniform Bi_2MoO_6 microplates transformed to uniform nanoplates of Bi_2MoO_6 structure due to the absorption of PEG on Bi_2MoO_6 nuclei that inhibited the nanocrystalline growth. It implies that the Bi_2MoO_6 nuclei grew in a two-dimensional (2D) mode to produce nanoplates [15].

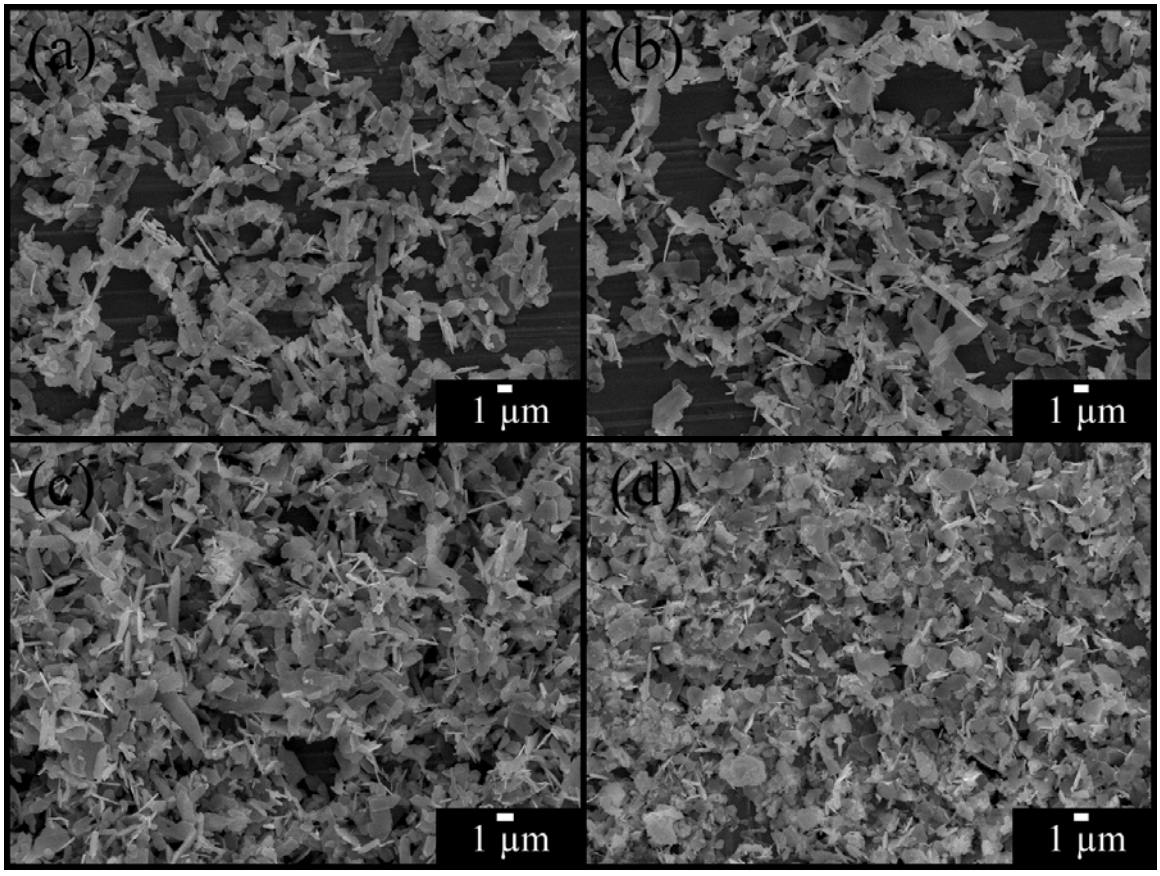

Fig. 2 SEM images of (a–d) Bi_2MoO_6 hydrothermally synthesized in the solutions containing 0.0, 0.1, 0.3 and 0.5 g PEG, respectively.

TEM images and SAED patterns of the products are shown in Fig. 3. They exhibit microplates of Bi_2MoO_6 in PEG-free solution and nanoplates of Bi_2MoO_6 for 0.5 g PEG adding. Selected area electron diffraction (SAED) patterns of individual Bi_2MoO_6 microplate and nanoplate show spot patterns which revealed single-crystalline nature. Moreover, the SAED patterns can be indexed as the (060), (062) and (002) planes in the [-100] zone axis of orthorhombic Bi_2MoO_6 structure, indicating the preferential growth unit cells along the b-axis.

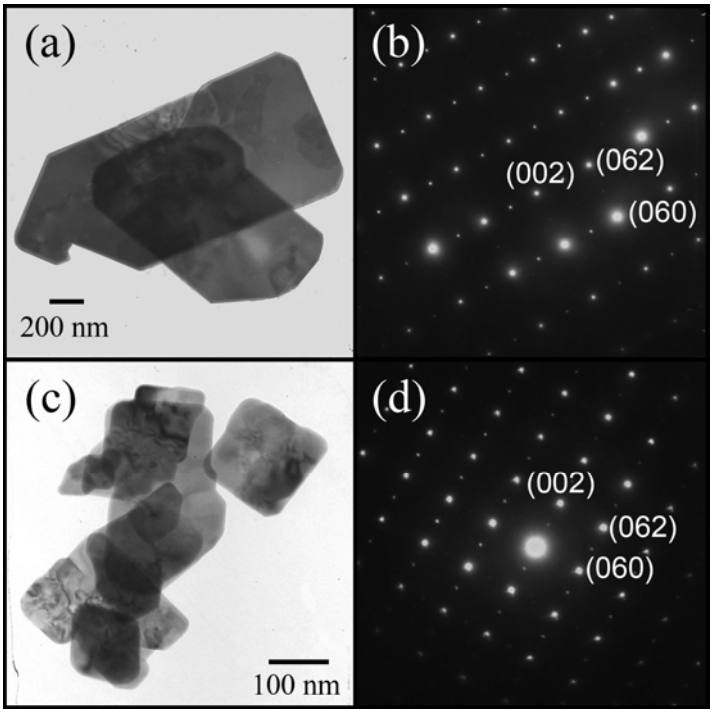

Fig. 3 TEM images and SAED patterns of Bi_2MoO_6 hydrothermally synthesized in (a, b) PEG-free solution and (c, d) the solution containing 0.5 g PEG.

The photocatalytic activities of Bi_2MoO_6 were investigated by the degradation of RhB under Xe lamp. Change in the UV-visible spectra of the aqueous RhB solutions using the Bi_2MoO_6 nanoplates is shown in Fig. 4. The highest absorption peak of RhB molecules at 553 nm rapidly decreased in intensity with exposure time under UV visible light. The absorbance of the suspension decreases with an associated wavelength shift of the band to higher energy with the presence of new band around 518 nm due to deethylation of RhB to rhodamine [5, 16], with changing in an initial red color to the final achromatic one. Degradation of RhB was almost complete when the exposure time reached at 180 min (results not shown).

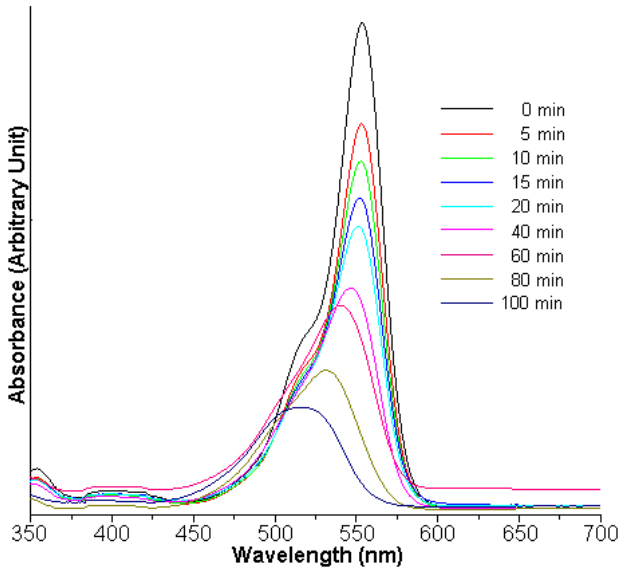

Fig. 4 UV-visible absorption of RhB solution containing Bi_2MoO_6 nanoplates hydrothermally synthesized in the solution containing 0.5 g PEG.

The photocatalytic degradation (C_t/C_0) of RhB on the Bi_2MoO_6 products is shown in Fig. 5a. It indicates that the Bi_2MoO_6 nanoplates have photocatalytic activities more than the Bi_2MoO_6 microplates. After 60 min of UV light exposure, about 68 % of RhB was degraded by using Bi_2MoO_6 nanoplates as catalyst, which is significantly larger than that of the Bi_2MoO_6 microplates (60 %). After 100 min, 95.02 % of RhB was degraded by Bi_2MoO_6 nanoplates. The results indicate that the as-synthesized Bi_2MoO_6 nanoplates exhibit an enhanced photocatalytic activity as compared to the Bi_2MoO_6 microplates.

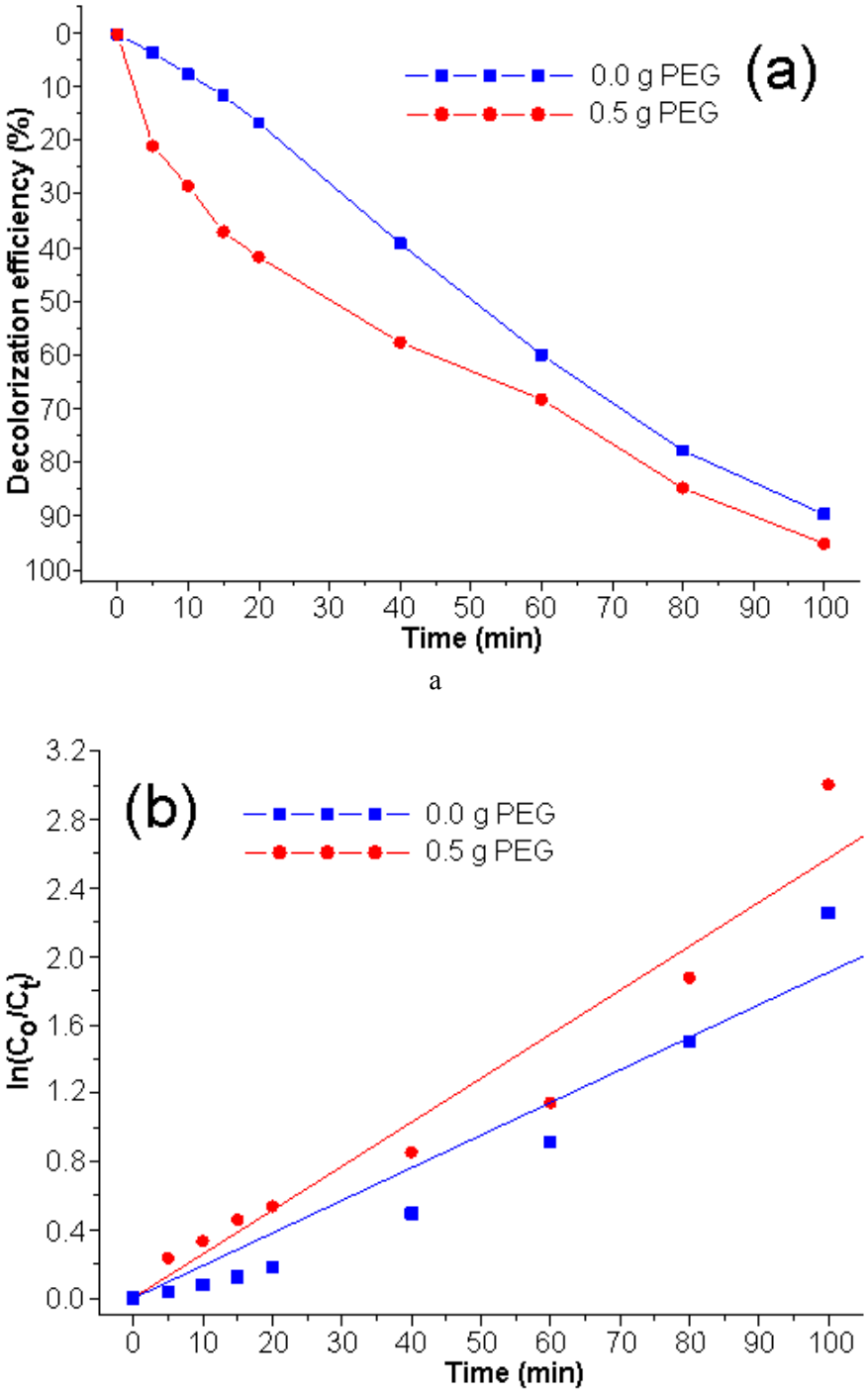

a

Fig. 5 (a) Decolorization efficiency and (b) $ln(C_o/C_t)$ for different lengths of UV visible irradiation time of Bi_2MoO_6 microplates and Bi_2MoO_6 nanoplates hydrothermally synthesized in the solutions with and without PEG.

The photocatalytic RhB degradation reaction was assumed to follow a pseudo-first-order kinetics [17–19] given by

$$\ln(C_0/C_t) = kt \quad (1)$$

where k is the apparent rate constant (min^{-1}), C_t is the solution-phase concentration of RhB, C_0 is the initial concentration at t = 0 and C_t/C_0 is the normalized organic compound concentration. The plots of $\ln(C_0/C_t)$ versus exposure time for the photodegradation of RhB (Fig. 5b) were in a linear line. In this research, the photodegradation followed very well with the pseudo-first order kinetics with $R^2 \rightarrow 1$ (0.9792 and 0.9700 for Bi_2MoO_6 microplates and Bi_2MoO_6 nanoplates) [18]. The value of k increases from 0.0207 to 0.0282 min^{-1} when the morphologies of Bi_2MoO_6 changed from microplates to nanoplates.

4. Conclusions

In conclusion, Bi_2MoO_6 nanoplates have been successfully synthesized via a simple hydrothermal method using polyethylene glycol with M.W. of 20,000 as surfactant. The orthorhombic Bi_2MoO_6 nanoplates show photocatalytic efficiency of 95.02 % for the degradation of RhB under the UV visible light illumination within 100 min.

Acknowledgments

We wish to thank the Thailand Office of the Higher Education Commission for providing financial support through the National Research University (NRU) Project for Chiang Mai University; the National Nanotechnology Center (NANOTEC), National Science and Technology Development Agency, for providing financial support through the project P-10-11345; and the Graduate School of Chiang Mai University through a general support.

References

[1] G. Yang, Q. Zhang, W. Chang, W. Yan, J. Alloy. Compd. **580**, 29 (2013).
[2] X. Xiao, R. Hu, C. Liu, C. Xing, X. Zuo, J. Nan, L. Wang, Chem. Eng. J. **225**, 790 (2013).
[3] J. Bi, J. Che, L. Wu, M. Liu, Mater. Res. Bull. **48**, 2071 (2013).
[4] K. Honda, A. Fujishima, Nature **238**, 37 (1972).
[5] H. Yu, Z. Zhu, J. Zhou, J. Wang, J. Li, Y. Zhang. Appl. Surf. Sci. **265**, 424 (2013).
[6] H.H. Li, C.Y. Liu, K. Li, H. Wang, J. Mater. Sci. **43**, 7026 (2008).
[7] P. Wang, Y. Ao, C. Wang, J. Hou, J. Qian, Carbon **50**, 5256 (2012).
[8] X. Zhao, T. Xu, W. Yao, Y. Zhu, Appl. Surf. Sci. **255**, 8036 (2009).
[9] H. Li, K.W. Li, H. Wang, Mater. Chem. Phys. **116**, 134 (2009).
[10] C. Xu, D. Zou, L. Wang, H. Luo, T. Ying, Ceram. Int. **35**, 2099 (2009).
[11] H. Xie, D. Shen, W. Wang, G. Shen, Mater. Chem. Phys. **110**, 332 (2008).
[12] Powder Diffract. File, JCPDS-ICDD, 12 Campus Boulevard, Newtown Square, PA 19073, U.S.A., (2001).
[13] L. Zhang, T. Xu, X. Zhao, Y. Zhu, Appl. Catal. B **98**, 138 (2010).
[14] C. Kongmark, R. Coulter, S. Cristol, A. Rubbens, C. Pirovano, A. Löfberg, G. Sankar, W.V. Beek, E.B. Richard, R.N. Vannier, Cryst. Growth. Des. **12**, 5994 (2012).
[15] W. Wang, X. Qiao, J. Chen, H. Li, Mater. Lett. **61**, 3218 (2007).
[16] H. Fu, S. Zhang, T. Xu, Y. Zhu, J. Chen, Environ. Sci. Technol. **42**, 2085 (2008).
[17] L. Liang, Y. Yulin, L. Xinrong, F. Ruiqing, S. Yan, L. Shuo, Z. Lingyun, F. Xiao, T. Pengxiao, X. Rui, Z. Wenzhi, W. Yazhen, M. Liqun, Appl. Surf. Sci. **265**, 36 (2013).
[18] O. Yayapao, T. Thongtem, A. Phuruangrat, S. Thongtem, Mater. Lett. **90**, 83 (2013).
[19] J. Chanathaworn, C. Bunyakan, W. Wiyaratn, J. Chungsiriporn, Songklanakarin J. Sci. Technol. **34**, 203 (2012).